

Measurements of gravity wave global distributions and trends in the ITM

Primary author: Mike J. Taylor: Center for Atmospheric and Space Sciences, Utah State University, 435-797-3919, mike.taylor@usu.edu

Co-authors: Katrina Bossert (Arizona State University), Rich Collins (University of Alaska-Fairbanks), Chihoko Cullens (University of Colorado - Boulder/Laboratory for Atmospheric and Space Physics), Aimee Merkel (University of Colorado - Boulder/Laboratory for Atmospheric and Space Physics), Tracy Moffat-Griffin (British Antarctic Survey), Pierre-Dominique Pautet (Center for Atmospheric and Space Sciences, Utah State University), Peter Preusse (Forschungszentrum Jülich), Gunter Stober (University of Bern & OCCR), Ed Thiemann (University of Colorado - Boulder/Laboratory for Atmospheric and Space Physics), Brentha Thurairajah (Virginia Tech), Titus Yuan (Center for Atmospheric and Space Sciences, Utah State University), Yucheng Zhao (Center for Atmospheric and Space Sciences, Utah State University)

Synopsis

Gravity waves (GWs) are the fundamental link that connects the tropospheric weather to the space weather. Hence, global measurements to characterize their parameters, distribution and main trends in the ITM are crucial. This white paper summarizes current GW measurement techniques operated from ground-based to space borne platforms. The capabilities and limitations of each technique are described and discussed. The gaps in current global GW measurements are identified and possible solutions are suggested.

1. Measurements required to determine the global distribution of GWs in the ITM

Traditionally gravity waves (GWs) have been understood to couple the troposphere, stratosphere, and mesosphere (0-90 km), where waves generated by meteorological processes in the troposphere propagate upward into the stratosphere and mesosphere, grow in amplitude until they are dissipated by breaking or wind blocking, and drive the circulation of the stratosphere and mesosphere (Fritts and Alexander, 2003; Yiğit & Medvedev, 2010; 2015). Over the past decade a variety of theoretical and observational studies have revealed that waves have a crucial role in coupling the thermosphere with the mesosphere, stratosphere and troposphere below and coupling space weather and terrestrial weather (or meteorology).

From ground-based sites and from airborne or space-based platforms, multiple techniques have been employed to support and guide the theoretical and modeling efforts. However, many GW characteristics and effects have yet to be quantified and understood. Current GW measurements have many limitations (wave spectrum, vertical, spatial, temporal distributions). We need to treat the atmosphere over a much larger scale to understand the bigger picture. In this case, the overarching unknowns comprise GW characteristics (scale sizes, period, propagation direction, and their associated energy and momentum fluxes) and distribution (global forcing, regional variations, seasonal and long-term variations), their effects on the background atmosphere (temperature, wind, composition, mixing), PWs or tides, and their coupling roles (between troposphere and middle/upper atmosphere, between neutral atmosphere and ionosphere, and in interhemispheric processes). Furthermore, the effects of tides and PWs on small-scale GW propagation and vice-versa GW forcing of these larger waves, are still not fully understood.

To address these pressing issues, ideally, the following measurements are required:

- Global measurements (covering the world, from ground to ~500 km),
- Simultaneous measurements of the background and the wave perturbations in wind, temperature (or a proxy such as airglow intensity), and density,
- Wave measurements comprising all scale sizes from ~10 to 1000s km in the horizontal, and from ~1 to ~100 km in the vertical, covering observed wave periods from 1 min to 24 hours,
- Simultaneous vertical and horizontal measurements of the same wave event, and its evolution (4D),
- Continuous daytime and nighttime observations,
- Seasonal and long-term observations (several years to possibly several solar cycles).

2. Overview of current technologies

To date, a broad range of instruments and techniques are utilized to measure the required parameters. The following sections briefly overview their capabilities and limitations.

2.1. Passive optical system

Naturally occurring airglow emissions (e.g., OH, O₂, Na, OI 5577, OI 6300) have successfully been used for several decades to study GWs in the ITM system (e.g., Taylor et al., 1995). These airglow layers spread from ~80 to ~250 km altitude. Passive imaging systems with field-of-view from a few degrees to all-sky (180°) allow measurements of GW horizontal

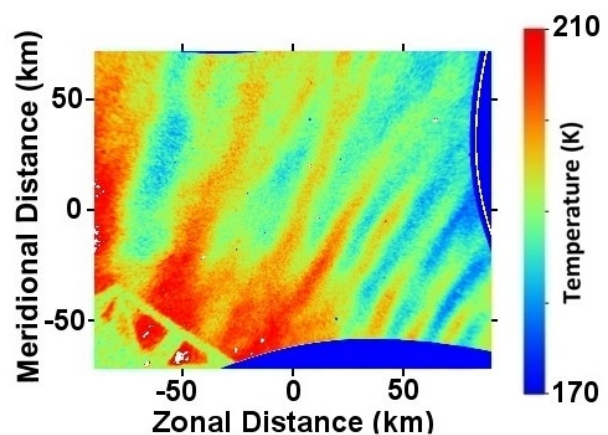


Figure 1: AMTM temperature map showing quasi-monochromatic GW at 87 km (Pautet et al., 2014).

characteristics (e.g., scale sizes, phase speed, direction, period, and perturbation amplitude) within each airglow layer (e.g., Taylor et al., 1997; Hecht et al., 2001; Ejiri et al., 2003; Suzuki et al., 2004; Nielsen et al., 2009). This technology is limited to nighttime measurements and to GWs with vertical wavelengths larger than the layer thickness. Recent detector and optical developments enable derivation of the temperature measurements of wave field perturbations, and background, important to quantify GW impacts (e.g., Ground-based Infrared P-branch Spectrometer, GRIPS, Pilger and Bittner, 2009; Advanced Mesospheric Temperature Mapper, AMTM, Figure 1, Pautet et al., 2014; Taylor et al., 2019). Likewise, airglow emissions are used to map 2D horizontal wind with interferometer instruments (e.g., Scanning Doppler Imager, Conde and Nicolls, 2010; Wind Imaging Interferometer, Kristoffersen et al., 2022).

Passive observations can also be made from space. For example, solar and stellar occultation at Far Ultraviolet (FUV) and Extreme Ultraviolet (EUV) use the extinction of sun or starlight to quantify the atmospheric column along the line of sight and have been used to characterize gravity waves by measuring their vertical wavelength and by fully constraining their potential energy flux, and partially constraining their momentum flux (Nakagawa et al. 2020, Starichenko, et al 2021). Likewise, infrared limb imaging measures temperature by thermal emissions of the atmosphere. Combined with tomography, GWs with horizontal wavelengths >80 km can be sounded in 3D from airplane (e.g., Krisch et al., 2017), and potentially from satellites in the future (Preusse et al., 2014).

2.2. Lidars

Lidars have continued to advance our understanding of the structure and dynamics of the middle and upper atmosphere (stratosphere-mesosphere-lower thermosphere) over the past decade (see recent review by She et al., 2021 and references therein). Rayleigh and resonance lidars yield measurements of vertical profiles of density, metal (i.e., Na, Fe, K) temperature, and/or wind by combining scattering from the neutral air (Rayleigh) and from atomic metals (resonance) with precision spectroscopic techniques. The most advanced systems provide common volume measurements of wind and temperature at high resolution in day and night. The collocation of Rayleigh and resonance lidars have provided continuous measurements from ~30 to 110 km that yield insights into the vertical coupling of the whole atmosphere through measurements of the propagation and breaking of waves and tides (e.g., Hildebrand et al., 2012; Li et al., 2021).

State of the art lidar systems have been established at a variety of observatories around the world. Rayleigh lidar measurements at McMurdo, Antarctica, have yielded measurements of secondary gravity wave generation in the mesosphere (Vadas et al., 2018; 2019). Iron resonance lidar measurements at McMurdo, Antarctica have revealed the presence of extended thermospheric layers, the presence of fast gravity waves in the thermosphere (Chu et al., 2011). The sodium resonance lidar observations at the Andes Lidar Observatory (ALO) at Cerro Pachon, Chile, has yielded measurements of horizontal tidal winds in the thermosphere, and wave-driven heat fluxes and turbulence in the mesosphere (Figure 2, Liu et al., 2016; Guo et al, 2017). Resonance lidar measurements at Utah State University, USA, have revealed changes in the circulation of the lower thermosphere driven by coronal mass ejections that may be a source of gravity waves (Yuan et al., 2015). The collocation of Rayleigh and resonance lidars have provided continuous measurements from ~30 to 110 km that yield insights into the vertical coupling of the whole atmosphere through measurements of the propagation and breaking of GWs and tides (e.g., Hildebrand et al., 2012; Li et al., 2021). Rayleigh and resonance lidar measurements coordinated with rocket soundings at Poker Flat Research Range, Alaska, have yielded measurements of waves and turbulence in the mesosphere (Triplett et al., 2018) and the thermodynamics of water in the lower thermosphere

(Collins et al., 2021). The Raman Lidar for Meteorological Observations (RALMO) at Payerne, Switzerland (Sica and Haefele, 2016), and the Purple Crow Lidar in London, Canada (Sica and Haefele, 2015, Jalali et al., 2019), benefiting from advanced in signal processing, are able to measure temperature, water vapor, and aerosol on a routine basis up to the lower mesosphere (RALMO, Stober et al., 2021a), or to reach altitudes up to 100 km (Purple Crow Lidar).

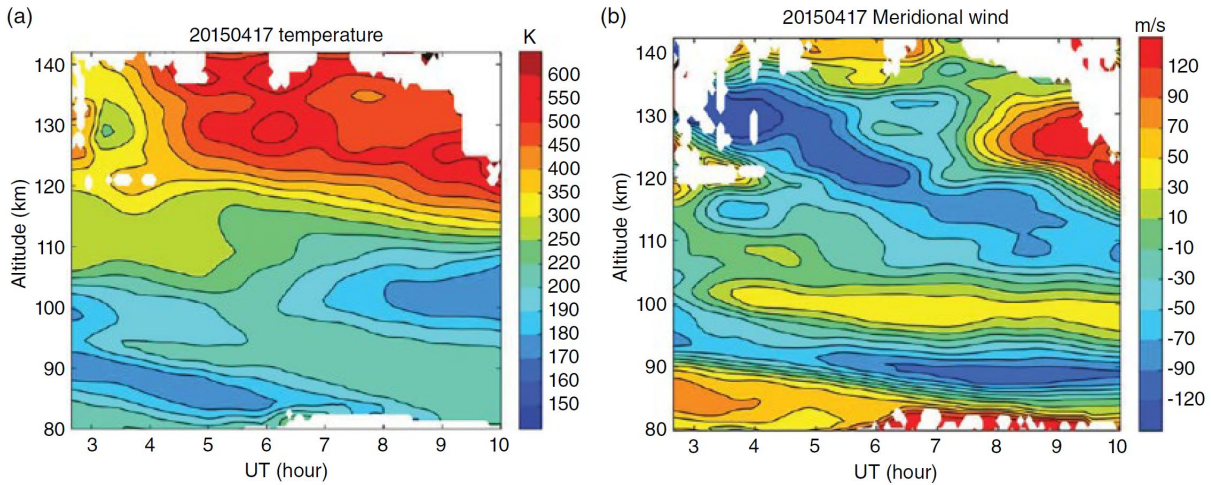


Figure 2: (a) Temperature and (b) meridional wind measured by the Na lidar at ALO on 17 April 2015. The existence of a thermospheric Na layer enabled measurements up to 140 km (She et al., 2021).

Continued advances in laser and optical technologies, especially diode laser and fiber laser technologies, have resulted in the upgrading of existing lidar systems to make them more robust and accurate, and the development of new systems that are portable and highly automated (Liu et al., 2016; Kawahara, et al., 2017; Xia et al., 2017; Li et al., 2020; Kaifler and Kaifler, 2021; Lübken and Höffner, 2021; Collins et al., 2022). These advances have also supported the development of lidars that can measure new species such as metastable Helium in the thermosphere (Kaifler et al., 2022). The development and success of ground-based and airborne systems have also prompted the design and development of resonance lidar systems for deployment in space to provide global views of the waves and the wave driven circulation (Janches et al., 2022).

2.3. Radars

Radars have become a widespread tool to measure mesospheric/lower thermospheric winds used to study the MLT dynamics including PWs, tides, and GWs. In particular, meteor radars take advantage of the continuous influx of meteoroids, creating ionized trails that drifts with the neutral wind (Hocking 1999; Hocking et al., 2001; Holdsworth et al., 2004). Currently, radars provide continuous and autonomous observations with a high degree of automated data analysis, and standard data products such as hourly horizontal winds, daily mean temperatures, and estimates of GW momentum fluxes for various scales (Hocking, 2005). They are distributed worldwide and currently cover latitudes from 79°N to 78°S, on almost all continents (see Figure 5).

A breakthrough was achieved with a new generation of higher power meteor radars such as the Southern Argentina Agile Meteor Radar (SAAMER) or the Trondheim system (Fritts et al., 2010a; 2010b; de Wit et al., 2016; 2017).

Recently, multi-static observations using networks of meteor radars, which are based on 2DVAR approaches, have become available as well (Walteufel and Corbin, 1979; Stober and Chau, 2015; Vierinen et al., 2016; Chau et al., 2017; Stober et al., 2018; Volz et al., 2021). The

current meteor radar networks performing continuous observations are the Nordic Meteor Radar Cluster, and the Chilean Observation Network De Meteor Radars (CONDOR, see Figure 3, Stober et al., 2021b; 2022). These new capabilities enable the investigation of horizontal wavelength spectra down to scales of 50-60 km for all three wind components, and measurements of momentum fluxes and wind variances at shorter time scales than what is achievable with standard monostatic systems.

2.4. LF-pulse sensing

LF-pulse sensing of the D-region has been recently employed to measure GWs in the upper atmosphere (Iwata and Ishikawa, 1974; Lay and Shao, 2011). This technique allows for measuring the vertical displacement of the bottom side of the ionosphere (80-90 km altitude). Waves with vertical wavelength from ~150 m to a few km, and a period over 6 s, can be measured over full 24 hours, but with a much lower ionospheric variability during daytime.

The majority of these instruments are currently ground-based, operating often simultaneously as clusters or networks to take advantage of their complementary measurement capabilities.

3. Observation platforms

3.1. Ground-based observations - Instrument clusters and networks

Figure 4 shows a map of the current main instrument clusters dedicated to aeronomy studies. Red dots correspond to sites with all three main types of instruments (passive optical system, lidar, radar), yellow dots correspond to sites with only two types of instruments.

To extend the coverage of a specific type of instrument, several networks have been established and are currently operational such as MANGO

(Mid-latitude All-sky imaging Network for Geospace Observations), ANGWIN (Antarctica GW Instrument Network), SuperDARN, Boston University mesospheric/thermospheric imagers, radar network... As an example, Figure 5 shows the network of meteor radars currently operating.

These instrument clusters and networks span a large latitude range but enormous gaps still exist such as the Oceans or the African continent.

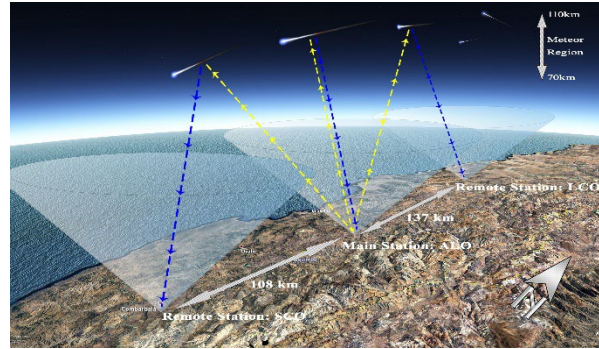


Figure 3: Illustration of the CONDOR multi-static meteor radar detection centered on the Andes Lidar Observatory, Chile.

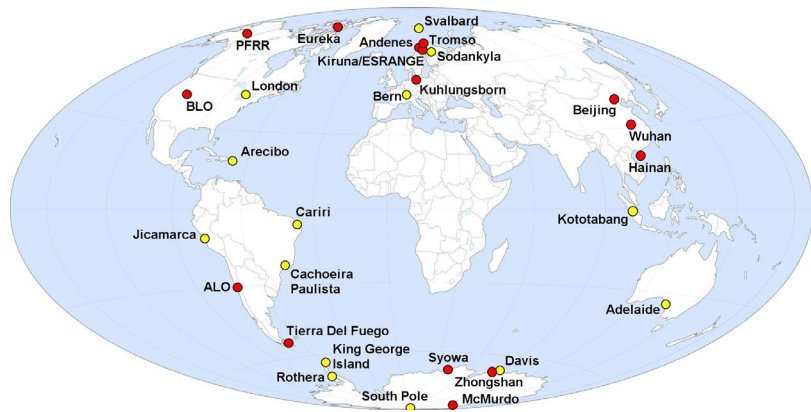


Figure 4: Current clusters of aeronomy instruments.



Figure 5: Global meteor radars network (courtesy S. Eckermann).

3.2. Airborne and space borne missions

Airborne platforms have been used for decades to study tropospheric weather and phenomenon, but it was only recently that several projects were designed to investigate GWs in the middle and upper atmosphere. Most notably, ALOHA-90 and ALOHA/ANLC-93 (Hostetler and Gardner, 1994; Gardner, 1995; Swenson et al., 1995), and recently DEEPWAVE (Fritts et al., 2016), GW_LCYCLE, or SOUTHTRAC (Rapp et al., 2021) employed airglow imagers, infrared limb imagers, and lidars onboard research aircrafts to cover large regions, usually inaccessible to ground-based instruments, and to characterize propagation through a large range of altitudes. Stratospheric balloons have also been used to make in-situ measurements in the middle atmosphere (e.g., Hertzog et al., 2012; Plougonven et al., 2013), or to remotely study the upper atmosphere (e.g., TurboPMC, Fritts et al., 2019).

Satellite missions have been launched since the 1990s to study the ITM system, such as UARS, SME (Clancy et al., 1994). They have employed two types of measurement techniques: nadir viewing (imager or lidar pointing directly towards the Earth), or limb scanning (optical instruments measuring the scattering of sunlight at the limb to obtain vertical profiles). Nadir viewing instruments are capable of measuring the horizontal wave characteristics over large areas, with global coverage, but with a coarser vertical resolution. The limb scanning instruments provide vertical profiles of various background fields and wave parameters, but are limited to larger horizontal wavelength waves (Wright et al., 2016). The current missions/instruments include AQUA/AIRS, AIM, CrIS, GOLD, ICON/MIGHTI, AURA/MLS (Waters et al., 2006), NIRAC, ODIN/OSIRIS, TIMED/SABER, COSMIC-2 and VIIRS. *Table 1* summarizes their capabilities and limitations on GW measurements. In the near future, new missions or instruments such as AWE (the first NASA dedicated GW mission, capable of temperature mapping and MF at OH layer altitude), DYNAGLO (dual cubesat measuring horizontal waves at 150 km), MATS (temperature profiles 75-110 km, NLC mapping, and 3D GW reconstruction, Gumbel et al., 2020), and OWLS (density profiles ~100-230 km, vertical waves, potential energy flux), will soon add new capabilities in GW observations and expand our knowledge on their characteristics.

Recent missions	Altitude range (km)	Latitude range (°)	Day/Night	Type	Resolution/Sampling (km)	Comments
AIM/CIPS	~50	+/- 75	Twilight	Nadir	10 Vert, 7.5 Horiz	Rayleigh Albedo Anomaly
	80-85	60-85 N and S				PMC
AIM/SOFIE	20-100	65-85 N and S	Day	Limb	2 Vert, 300 Horiz	
AQUA/AIRS	35-40	+/- 85	Day and night	Nadir	6-10 Vert, 30 Horiz	Sun-synchronous
AURA/MLS	10-90	+/- 82	Day and night	Limb	4-10 Vert, 165 Horiz	Sun-synchronous
COSMIC-2	0-60	+/- 24	Day and night	Limb	<1	
CrIS	35-40	+/- 85	Day and night	Nadir	10 Vert, 14 Horiz	Sun-synchronous
GOLD	140-180	+/- 60	Day	Nadir	40 Vert	Geostationary
ICON/MIGHTI	Night 94-110 and 230-270, day 94-280	-10 to +40	Day and night	Limb	> 500 Horiz	Wind
	Night 90-105, day 90-127					Temperature
NIRAC	~87	+/- 53	Night	Nadir	0.07 Horiz	OH brightness
ODIN/OSIRIS	7-65	+/- 82 but seasonal	Day	Limb	1 Vert	Sun-synchronous
TIMED/SABER	20-110	82N-52S or 52N-82S	Day and night	Limb	2.5 Vert, 100 Horiz	Temperature
VIIRS	~87	+/- 85	Night	Nadir	10 Vert, 0.75 Horiz	OH brightness
Future missions						
AWE	~87	+/- 53	Night	Nadir	30-300 Horiz	OH temperature
DYNAGLO	150 km	+/- 86	Day	Nadir	330 km Horiz	O/N ₂ density variations
MATS/Limb	75-110	Global	Day and night	Limb	1 Vert x 20 Horiz	O ₂ temperature
MATS/Nadir	80-86	45-90 N and S (NLC) Global (O ₂)	Day (NLC)/night (O ₂)	Nadir	0.5 vertx10 Horiz,	NLC and O ₂ nightglow
OWLS	100-230	~50 to 90 N and S	Dawn/dusk	Limb	<60 Vert	O ₂ density

Table 1: Capabilities and limitations of the current and near-future aeronomy missions.

Space-based instruments offer a much large geographical coverage, can measure vertical or horizontal GW wavelengths, with long-duration observations, but investigation of the lifecycle of individual GW events is more limited. Furthermore, depending on the orbits, it is difficult to properly assess the modal composition of the contributing tidal and PW fields.

4. Gaps in global measurements of GWs

The current or near-future aeronomy projects will provide a broad wealth of data that will significantly improve our knowledge on GW dynamics. Nevertheless, numerous gaps in these global measurements will still exist:

- As shown in *Table 1*, no individual instrument can cover all the GW scale sizes, both horizontally

and vertically, leaving gaps in the wave spectrum. In particular, the detectability of small-amplitude waves is limited due to instrument specifications, background noise, or low signal level. As they propagate to higher altitudes, those waves will grow larger and impact the atmosphere above the measurement region,

- Even space-borne missions are limited in coverage by their orbit, which results in missing regions, especially at high latitudes where ground-based measurements are already sparse,
- Simultaneous vertical and horizontal measurements of the same wave events are rare but essential to characterize GW without making any assumptions on their dynamics; ideally, these observations are carried out to provide full 3D/4D data fields,
- Simultaneous measurements of the neutral atmosphere and ion/electron content are necessary to understand the coupling between the mesosphere/thermosphere and the overlying ionosphere,
- Even though some missions have acquired data for many years, longer term measurements are essential to better understand the broader effects of phenomenon like El Niño, La Niña, or the solar cycle on GW dynamics (Beig et al., 2003).

5. Possible solutions

Newly available technologies and simultaneous operation of complementary instruments can provide possible solutions to fill the current measurement gaps. The following suggestions should be taken into consideration:

- The development/expansion of ground-based cluster/networks with recent high-resolution instruments such as AMTM, wind imaging interferometers, new generation high-power radars and lidars, spread out around the world, to establish global, simultaneous, multi-dimensional measurements of both the waves and background fields,
- Constellations of complementary satellite measurements with both wave and background temperature and wind fields, possibly using a combination of large satellites together with a suite of cubesats,
- Clear strategy to replace end-of-life satellites/instruments to assure continuity for long-term measurements,
- Take advantage of new space technologies such as infrared limb imaging to measure wind and temperature from 20 up to 250 km or to generate 3D distributions along the orbital track, or sub-limb imaging to observe very short wavelength waves in the mid-stratosphere,
- For space borne instruments, develop adequate observation strategy, such as deploying multiple satellites, to ensure a good time coverage of the upper atmospheric wind/temperature fields to better resolve tidal modes and account for two-way interaction between the background and GWs,
- Organize simultaneous coordinated GW and background measurements from the global ground-based networks and the satellite missions,
- Finally, cooperation with numerical models, including assimilation (Eckermann et al., 2018; Stober et al., 2020), is crucial to better understand the dynamics and effects of GWs in the Earth's or other planets' atmosphere.

The future DYNAMIC mission, which proposes to combine measurements from two satellites to delineate the dynamical behavior and structure of the ionosphere, thermosphere and mesosphere system, is an essential step in the right direction.

No instrument can do everything. However, we are now in an era when we can define the measurements we need and then achieve them!

References

Beig G., P. Keckhut, R. P. Lowe, R. G. Roble, M. G. Mlynczak, J. Scheer, V. I. Fomichev, D. Offermann, W. J. R. French, M. G. Shepherd, A. I. Semenov, E. E. Remsberg, C. Y. She, F. J. Lübken, J. Bremer, B. R. Clemesha, J. Stegman, F. Sigernes, and S. Fadnavis, Review of mesospheric temperature trends, *Reviews of Geophysics*, **41**, 4/1015, 2003

Chau, J. L., Stober, G., Hall, C. M., Tsutsumi, M., Laskar, F. I., & Hoffmann, P., Polar mesospheric horizontal divergence and relative vorticity measurements using multiple specular meteor radars, *Radio Science*, **52**(7), 811–828, <https://doi.org/10.1002/2016RS006225>, 2017

Chu, X., Z. Yu, C. S. Gardner, C. Chen, and W. Fong, Lidar observations of neutral Fe layers and fast gravity waves in the thermosphere (110–155 km) at McMurdo (77.8°S, 166.7°E), Antarctica, *Geophysical Research Letters*, **38**, 23, 2011

Clancy, R. T., Rush, D. W., & Callan, M. T., Temperature minima in the average thermal structure of the middle atmosphere (70–80 km) from analysis of 40- to 92-km SME global temperature profiles, *Journal of Geophysical Research*, **99**(D9), 19,001–19,020, <https://doi.org/10.1029/94JD01681>, 1994

Collins, R. L., J. Li, B. Williams, B. Kaifler, and D. Thorsen, All-Solid State Iron Resonance Lidar for Measurement of Temperature and Winds in the Upper Mesosphere and Lower Thermosphere, *Thirtieth International Laser Radar Conference*, Big Sky (Virtual), USA, 26 June - 1 July, 2022
Conde, M. G., and M. J. Nicolls, Thermospheric temperatures above Poker Flat, Alaska, during the stratospheric warming event of January and February 2009, *Journal of Geophysical Research*, **115**, D00N05, <https://doi:10.1029/2010JD014280>, 2010

Collins, R. L., M. H. Stevens, I. Azeem, M. J. Taylor, M. F. Larsen, B. P. Williams, J. Li, J. H. Alspach, P. -D. Pautet, Y. Zhao, and X. Zhu, Cloud formation from a localized water release in the upper mesosphere: Indication of rapid cooling, *Journal of Geophysical Research: Space Physics*, **126**, e2019JA027285, <https://doi:10.1029/2019JA027285>, 2021

Collins, R. L., J. Li, B. Williams, B. Kaifler, and D. Thorsen, All-Solid State Iron Resonance Lidar for Measurement of Temperature and Winds in the Upper Mesosphere and Lower Thermosphere, *Thirtieth International Laser Radar Conference*, Big Sky (Virtual), USA, 26 June - 1 July, 2022

de Wit, R. J., Janches, D., Fritts, D. C., & Hibbins, R. E., QBO modulation of the mesopause gravity wave momentum flux over Tierra del Fuego, *Geophysical Research Letters*, **43**(8), 4049–4055, <https://doi.org/10.1002/2016GL068599>, 2016

de Wit, R. J., Janches, D., Fritts, D. C., Stockwell, R. G., & Coy, L., Unexpected climatological behavior of MLT gravity wave momentum flux in the lee of the Southern Andes hot spot, *Geophysical Research Letters*, **44**(2), 1182–1191, <https://doi.org/10.1002/2016GL072311>, 2017

Eckermann, S. D., Ma, J.; Hoppel, K. W.; Kuhl, D. D.; Allen, D. R.; et al., High-Altitude (0–100 km) Global Atmospheric Reanalysis System: Description and Application to the 2014 Austral Winter of the Deep Propagating Gravity Wave Experiment (DEEPWAVE), *Monthly Weather Review*, Washington, **146**, 8, 2639-2666, <https://doi:10.1175/MWR-D-17-0386.1>, 2018

Ejiri, M.K., Shiokawa, K., Ogawa, T., Igarashi, K., Nakamura, T., and Tsuda, T., Statistical study of short-period gravity waves in OH and OI nightglow images at two separated sites, *Journal of Geophysical Research*, **108**(D21), 4679, 2003

Fritts, D. C., and M. J. Alexander, Gravity wave dynamics and effects in the middle atmosphere, *Review of Geophysics*, **41**, 1003, <https://doi:10.1029/2001RG000106>, 2003

Fritts, D. C., Janches, D., Jimura, H., Hocking, W. K., Mitchell, N. J., Stockwell, R. G., et al., Southern Argentina agile meteor radar: System design and initial measurements of large-scale winds and tides, *Journal of Geophysical Research*, **115**(D18), <https://doi.org/10.1029/2010JD013850>, 2010a

Fritts D. C., D. Janches, and W. K. Hocking, Southern Argentina Agile Meteor Radar: Initial assessment of gravity wave momentum fluxes, *Journal of Geophysical Research*, **115**, D19123, <https://doi:10.1029/2010JD013891>, 2010b

Fritts D.C., Smith R.B., Taylor M.J., Doyle J.M., Eckermann S.E., Dörnbrack A., Rapp M., Williams B.P., Pautet P.-D., Bossert K., Criddle N.R., Reynolds C.A., Reineke A., Uddstrom M., Revell M.J., Turner R., Kaifler B., Wagner J.S., Mixa T., Kruse C.G., Nugent A.D., Watson C.D., Gisinger S., Smith S.M., Moore J.J., Brown W.O., Haggerty J.A, Rockwell A., Stossmeister G.J., Williams S.F., Hernandez G., Murphy D.J., Klekociuk A., Reid I.M., and Ma J., The Deep Propagating Gravity Wave Experiment (DEEPWAVE): An airborne and ground-based exploration of gravity wave propagation and effects from their sources throughout the lower and middle atmosphere, *Bulletin of the American Meteorological Society*, <https://doi:10.1175/BAMS-D-14-00269.1>, 2016

Fritts, D. C., Miller, A. D., Kjellstrand, C. B., Geach, C., Williams, B. P., Kaifler, B., et al., PMC Turbo: Studying gravity wave and instability dynamics in the summer mesosphere using polar mesospheric cloud imaging and profiling from a stratospheric balloon, *Journal of Geophysical Research: Atmospheres*, **124**, 6423–6443, <https://doi.org/10.1029/2019JD030298>, 2019

Gardner, C.S., Introduction to ALOHA/ANLC-93: The 1993 airborne lidar and observations of the Hawaiian airglow/airborne noctilucent cloud campaigns, *Geophysical Research Letters*, **22**, 20, 2789-2792, <https://doi.org/10.1029/95GL02782>, 1995

Gumbel J., L. Megner., O. M. Christensen, S. Chang, J. Dillner, T. Ekebrand, G. Giono, A. Hammar, J. Hedin, N. Ivchenko, B. Karlsson, M. Kruse, A. Li, S. McCallion, D. P. Murtagh, G. Olentšenko, S. Pak, W. Park, J. Rouse, J. Stegman, G. Witt, The MATS Satellite Mission – Gravity Waves Studies by Mesospheric Airglow/Aerosol Tomography and Spectroscopy, *Atmospheric Chemistry and Physics*, <https://doi.org/10.5194/acp-2018-1162>, 2020

Guo, Y., A. Z. Liu, C. S. Gardner, First Na lidar measurements of turbulence heat flux, thermal diffusivity, and energy dissipation rate in the mesopause region, *Geophysical Research Letters*, **44**, 11, <https://doi.org/10.1002/2017GL073807>, 2017

Hecht, J.H., Walterscheid, R.L., Hickey, M.P., Franke, S.J., Climatology and modeling of quasi-monochromatic atmospheric gravity waves observed over Urbana Illinois, *Journal of Geophysical Research*, **106**(D6), 5181–5195, 2001

Hertzog, A., M. J. Alexander, and R. Plougonven, On the intermittency of gravity wave momentum flux in the stratosphere, *Journal of Atmospheric Sciences*, **69**(11), 3433–3448, 2012

Hildebrand, J., G. Baumgarten, J. Fiedler, U.-P. Hoppe, B. Kaifler, F.-J. Lübken, and B. P. Williams, Combined wind measurements by two different lidar instruments in the Arctic middle atmosphere, *Atmospheric Measurement Techniques*, **5**, 2433–2445, <https://doi.org/10.5194/amt-5-2433-2012>, 2012

Hocking, W.K., Temperatures using radar-meteor decay times, *Geophysical Research Letters*, **26**, 3297–3300, 1999

Hocking, W.K., A new approach to momentum flux determinations using SKiYMET meteor radars, *Annales Geophysicae*, **23**, 2433–2439, <https://doi.org/10.5194/angeo-23-2433-2005>, 2005

Hocking, W.K., B. Fuller, B. Vandepuer, Real-time determination of meteor-related parameters utilizing modern digital technology, *Journal of Atmospheric and Solar-Terrestrial Physics*, **63**, 2–3, 155-169, ISSN 1364-6826, [https://doi.org/10.1016/S1364-6826\(00\)00138-3](https://doi.org/10.1016/S1364-6826(00)00138-3), 2001

Holdsworth, D. A., I. M. Reid, and M. A. Cervera, Buckland Park all-sky interferometric meteor radar, *Radio Science*, **39**, RS5009, <https://doi:10.1029/2003RS003014>, 2004

Hostetler, C. A., and C. S. Gardner, Observations of horizontal and vertical wave number spectra of gravity wave motions in the stratosphere and mesosphere over the mid-Pacific, *Journal of Geophysical Research*, **99**, 1283-1302, 1994

Iwata, A., and H. Ishikawa, Lower Ionospheric Sounding by the Use of Loran-C Signals, *Journal of Geomagnetism and Geoelectricity*, **26**, 511-514, 1974

Jalali, A., S. Hicks-Jalali, R. J. Sica, A. Haeferle, and T. von Clarmann, A practical information-centered technique to remove a priori information from lidar optimal-estimation-method retrievals, *Atmospheric Measurement Techniques*, **12**, 3943–3961, <https://doi.org/10.5194/amt-12-3943-2019>, 2019

Janches, D., W. Yu, M. A. Krainak, C. Gardner, B. Kaifler, S. Etemad, D. C. Fritts, S. D. Eckermann, R. L. Collins, E. C. M. Dawkins, R. S. Lieberman, D. R. Marsh, G. Liu. and W. Jarvis, The Atmospheric

Coupling and Dynamics Across the Mesopause (ACaDAME) mission, *Advances in Space Research*, **64**(10), <https://doi.org/10.1016/j.asr.2019.07.012>, 2019

Kaifler, B., Ch. Geach, H. C. Budenbender, A. Mezger, and M. Rapp, Measurements of metastable helium in Earth's atmosphere by resonance lidar, under review, 2022

Kaifler, B. and N. Kaifler, A Compact Rayleigh Autonomous Lidar (CORAL) for the middle atmosphere, *Atmospheric Measurement Techniques*, **14**, 1715–1732, <https://doi.org/10.5194/amt-14-1715-2021>, 2021

Kawahara, T. D., S. Nozawa, N. Saito, T. Kawabata, T. T. Tsuda, and S. Wada, Sodium temperature/wind lidar based on laser-diode-pumped Nd:YAG lasers deployed at Tromsø, Norway (69.6°N, 19.2°E), *Optics Express*, **25**, A491-A501, 2017

Krisch, I., P. Preusse, J. Ungermann, A. Dörnbrack, S. D. Eckermann, M. Ern, F. Friedl-Vallon, M. Kaufmann, H. Oelhaf, M. Rapp, C. Strube, and M. Riese, First tomographic observations of gravity waves by the infrared limb imager GLORIA, *Atmospheric Chemistry and Physics*, **17**, 14937–14953, <https://doi.org/10.5194/acp-17-14937-2017>, 2017

Kristoffersen, S.K., W. E. Ward, J. Langille, W. A. Gault, A. Power, I. Miller, A. Scott, D. Arsenault, M. Favier, V. Losier, S. Lu, R. Zhang, and C. Zhang, Wind imaging using simultaneous fringe sampling with field-widened Michelson interferometers, *Applied Optics*, **61**, 6627-6641, <https://opg.optica.org/ao/abstract.cfm?URI=ao-61-22-6627>, 2022

Lay, E. H., and X.-M. Shao, High temporal and spatial-resolution detection of D-layer fluctuations by using time-domain lightning waveforms, *Journal of Geophysical Research*, **116**, A01317, <https://doi.org/10.1029/2010JA016018>, 2011

Li, J., B. P. Williams, J. H. Alspach, and R. L. Collins, Sodium Resonance Wind-Temperature Lidar at PFRR: Initial Observations and Performance, *Atmosphere*, **11**, <https://doi.org/10.3390/atmos11010098>, 2020

Liu, A. Z., Guo, Y., Vargas, F., & Swenson, G. R., First measurement of horizontal wind and temperature in the lower thermosphere (105–140 km) with a Na Lidar at Andes Lidar Observatory, *Geophysical Research Letters*, **43**, 2374–2380, <https://doi.org/10.1002/2016GL068461>, 2016

Lübken, F-J, and J. Höffner, VAHCOLI, a new concept for lidars: technical setup, science applications, and first measurements, *Atmospheric Measurement Techniques*, **14**, 3815–3836, <https://doi.org/10.5194/amt-14-3815-2021>, 2021

Nakagawa, H., et al., Vertical propagation of wave perturbations in the middle atmosphere on Mars by MAVEN/IUVS, *Journal of Geophysical Research: Planets*, **125**, 9, <https://doi.org/10.1029/2020JE006481>, 2020

Nielsen, K., M.J. Taylor, R.E. Hibbins, and M.J. Jarvis, Climatology of short-period mesospheric gravity waves over Halley, Antarctica (76S, 27W), *Journal of Atmospheric and Solar-Terrestrial Physics*, **71**, 991–1000, 2009

Pautet, P.-D., Taylor, M. J., Pendleton, W. R., Zhao, Y., Yuan, T., Esplin, R., & McLain, D., Advanced mesospheric temperature mapper for high-latitude airglow studies, *Applied Optics*, **53**(26), 5934–5943, <https://doi.org/10.1364/ao.53.005934>, 2014

Pilger, C., and M. Bittner, Infrasound from tropospheric sources: impact on mesopause temperature, *Journal of Atmospheric and Solar-Terrestrial Physics*, 816–822, 2009

Plougonven, R., A. Hertzog, and L. Guez, Gravity waves over Antarctica and the Southern Ocean: Consistent momentum fluxes in mesoscale simulations and stratospheric balloon observations, *Quarterly Journal of the Royal Meteorological Society*, **139**(670), 101–118, <https://doi.org/10.1002/qj.1965>, 2013

Preusse, P., M. Ern, P. Bechtold, S. D. Eckermann, S. Kalisch, Q. T. Trinh, and M. Riese, Characteristics of gravity waves resolved by ECMWF, *Atmospheric Chemistry and Physics*, **14**, 19, 10,483-10,508, <https://doi.org/10.5194/acp-14-10483-2014>, 2014

Rapp, M., B. Kaifler, A. Dörnbrack, S. Gisinger, T. Mixa, R. Reichert, N. Kaifler, S. Knobloch, R. Eckert, N. Wildmann, A. Giez, L. Krasauskas, P. Preusse, M. Geldenhuys, M. Riese, W. Woiwode, F. Friedl-Vallon, B.-M. Sinnhuber, A. de la Torre, P. Alexander, J. L. Hormaechea, D. Janches, M. Garhammer, J. L. Chau, J. F. Conte, P. Hoor, and A. Engel, SOUTHTRAC-GW An Airborne Field Campaign to Explore Gravity Wave Dynamics at the World's Strongest Hotspot, *Bulletin of the American Meteorological Society*, **104**, 4, <https://doi.org/10.1175/BAMS-D-20-0034.1>, 2021

She, C.-Y., Liu, A.Z., Yuan, T., Yue, J., Li, T., Ban, C. and Friedman, J.S., MLT Science Enabled by Atmospheric Lidars, In *Upper Atmosphere Dynamics and Energetics* (eds W. Wang, Y. Zhang and L.J. Paxton), <https://doi.org/10.1002/9781119815631.ch20>, 2021

Sica, R.J., A. Haefele, Retrieval of temperature from a multiple-channel Rayleigh-scatter lidar using an optimal estimation method, *Applied Optics*, **54**(8), 1872-89, <https://doi.org/10.1364/AO.54.001872>, 2015

Sica, R.J., and A. Haefele. Retrieval of water vapor mixing ratio from a multiple channel Raman-scatter lidar using an optimal estimation method, *Applied Optics*, **55** (4), 2016

Starichenko, E.D., et al., Gravity wave activity in the Martian atmosphere at altitudes 20–160 km from ACS/TGO occultation measurements, *Journal of Geophysical Research: Planets*, **126**, 8, <https://doi.org/10.1029/2021JE006899>, 2021

Stober, G., and J. L. Chau, A multistatic and multi frequency novel approach for specular meteor radars to improve wind measurements in the MLT region, *Radio Science*, **50**, 431–442, <https://doi.org/10.1002/2014RS005591>, 2015

Stober, G., Chau, J. L., Vierinen, J., Jacobi, C., and Wilhelm, S., Retrieving horizontally resolved wind fields using multi-static meteor radar observations, *Atmospheric Measurement Techniques*, **11**, 4891–4907, <https://doi.org/10.5194/amt-11-4891-2018>, 2018

Stober, G., Baumgarten, K., McCormack, J. P., Brown, P., and Czarnecki, J., Comparative study between ground-based observations and NAVGEM-HA analysis data in the mesosphere and lower thermosphere region, *Atmospheric Chemistry and Physics*, **20**, 11979–12010, <https://doi.org/10.5194/acp-20-11979-2020>, 2020

Stober, G., Janches, D., Matthias, V., Fritts, D. C., Marino, J., Moffat-Griffin, T., Baumgarten, K., Lee, W., Murphy, D., Kim, Y. H., Mitchell, N., and Palo, S., Seasonal evolution of winds, atmospheric tides, and Reynolds stress components in the Southern Hemisphere mesosphere–lower thermosphere in 2019, *Annales Geophysicae*, **39**, 1–29, <https://doi.org/10.5194/angeo-39-1-2021>, 2021a

Stober, G., Kozlovsky, A., Liu, A., Qiao, Z., Tsutsumi, M., Hall, C., Nozawa, S., Lester, M., Belova, E., Kero, J., Espy, P. J., Hibbins, R. E., and Mitchell, N.: Atmospheric tomography using the Nordic Meteor Radar Cluster and Chilean Observation Network De Meteor Radars: network details and 3D-Var retrieval, *Atmospheric Measurement Techniques*, **14**, 6509–6532, <https://doi.org/10.5194/amt-14-6509-2021>, 2021b

Stober, G., Liu, A., Kozlovsky, A., Qiao, Z., Kuchar, A., Jacobi, C., Meek, C., Janches, D., Liu, G., Tsutsumi, M., Gulbrandsen, N., Nozawa, S., Lester, M., Belova, E., Kero, J., and Mitchell, N.: Meteor Radar vertical wind observation biases and mathematical debiasing strategies including a 3DVAR+DIV algorithm, *EGUsphere preprint*, <https://doi.org/10.5194/egusphere-2022-203>, 2022

Suzuki, S., Shiokawa, K., Otsuka, Y., Ogawa, T., and Wilkinson, P., Statistical characteristics of gravity waves observed by an all-sky imager at Darwin, Australia, *Journal of Geophysical Research*, **109**, D20S07, 2004

Swenson, G. R., M. J. Taylor, P. J. Espy, C. S. Gardner, and X. Tao, ALOHA-93 measurements of intrinsic AGW characteristics using airborne airglow imager and ground based Na wind/temperature lidar, *Geophysical Research Letters*, **22**, 2841, 1995

Taylor, M.J., M.B. Bishop, and V. Taylor, All-sky measurements of short period waves imaged in the OI(557.7 nm), Na(559.2 nm) and near infrared OH and Oz(0,1) nightglow emissions during the ALOHA-93 campaign, *Geophysical Research Letters*, **22**, 2833–2836, 1995

Taylor, M.J., Pendleton Jr., W.R., Clark, S., Takahashi, H., Gobbi, D., and Goldberg, R.A., Image measurements of short-period gravity waves at equatorial latitudes, *Journal of Geophysical Research*, **102**(D22), 26283–26299, 1997

Taylor, M. J., Pautet, P.-D., Fritts, D. C., Kaifler, B., Smith, S. M., Zhao, Y., et al., Large-amplitude mountain waves in the mesosphere observed on 21 June 2014 during DEEPWAVE: 1. Wave development, scales, momentum fluxes, and environmental sensitivity, *Journal of Geophysical Research: Atmospheres*, **124**, <https://doi.org/10.1029/2019JD030932>, 2019

Triplett, C. C., J. Li, R. L. Collins, G. A. Lehmacher, A. Barjatya, D. C. Fritts, B. Strelnikov, F.-J. Lübken, B. Thurairajah, V. L. Harvey, D. L. Hampton, and R. H. Varney, Observations of Reduced Turbulence and Wave Activity in the Arctic Middle Atmosphere Following the January 2015 Sudden Stratospheric Warming, *Journal of Geophysical Research: Atmosphere*, **123**, 23, <https://doi.org/10.1029/2018JD028788>, 2018

Vadas, S. L., Zhao, J., Chu, X., & Becker, E., The excitation of secondary gravity waves from local body forces: Theory and observation, *Journal of Geophysical Research: Atmospheres*, **123**, 9296–9325, <https://doi.org/10.1029/2017JD027970>, 2018

Vadas, S. L., S. Xu, J. Yue, K. Bossert, E. Becker, and G. Baumgarten, Characteristics of the quiet-time hot spot gravity waves observed by GOCE over the Southern Andes on 5 July 2010, *Journal of Geophysical Research*, **124**, 7034–7061, <https://doi.org/10.1029/2019JA026693>, 2019

Vierinen, J., Chau, J. L., Pfeffer, N., Clahsen, M., and Stober, G., Coded continuous wave meteor radar, *Atmospheric Measurement Techniques*, **9**, 829–839, <https://doi.org/10.5194/amt-9-829-2016>, 2016

Volz, R., J. L. Chau, P. J. Erickson, J. P. Vierinen, J. M. Urco, and M. Clahsen, Four-dimensional mesospheric and lower thermospheric wind fields using Gaussian process regression on multistatic specular meteor radar observations, *Atmospheric Measurement Techniques*, **14**, 7199–7219, <https://doi.org/10.5194/amt-14-7199-2021>, 2021

Waters, J.W., The Earth observing system microwave limb sounder (EOS MLS) on the aura Satellite, *IEEE Transactions on Geoscience and Remote Sensing*, **44**, 5, 1075-1092, <https://doi:10.1109/TGRS.2006.873771>, 2006

Waldteufel, P. and Corbin, H., On the Analysis of Single-Doppler Radar Data, *Journal of Applied Meteorology and Climatology*, **18**, 4, 532-542, 1979

Wright, C. J., N. P. Hindley, A. C. Moss, and N. J. Mitchell, Multi-instrument gravity-wave measurements over Tierra del Fuego and the Drake Passage – Part 1: Potential energies and vertical wavelengths from AIRS, COSMIC, HIRDLS, MLS-Aura, SAAMER, SABER and radiosondes, *Atmospheric Measurement Techniques*, **9**, 877–908, <https://doi.org/10.5194/amt-9-877-2016>, 2016

Xia, Y., L. Du, X. Cheng, F. Li, J. Wang, Z. Wang, Y. Yang, X.Lin, Y. Xun, S. Gong, and G. Yang, Development of a solid-state sodium Doppler lidar using an all-fiber-coupled injection seeding unit for simultaneous temperature and wind measurements in the mesopause region, *Optics Express*, **25**, 5264-5278, 2017

Yiğit, E., and A. S. Medvedev, Internal gravity waves in the thermosphere during low and high solar activity: Simulation study, *Journal of Geophysical Research*, **115**, A00G02, <https://doi:10.1029/2009JA015106>, 2010

Yiğit, E., and A. S. Medvedev, Internal wave coupling processes in Earth's atmosphere, *Adv. Space Res.*, **55**, 983– 1003, <https://doi:10.1016/j.asr.2014.11.020>, 2015

Yuan, T., Zhang, Y., Cai, X., She, C.-Y., and Paxton, L. J., Impacts of CME-induced geomagnetic storms on the midlatitude mesosphere and lower thermosphere observed by a sodium lidar and TIMED/GUVI, *Geophysical Research Letters*, **42**, 7295– 7302, <https://doi:10.1002/2015GL064860>, 2015

Yuan, T., Solomon, S. C., She, C.-Y., Krueger, D. A., & Liu, H.-L., The long-term trends of nocturnal mesopause temperature and altitude revealed by Na lidar observations between 1990 and 2018 at mid-latitude, *Journal of Geophysical Research: Atmospheres*, **124**, 5970–5980, <https://doi.org/10.1029/2018JD029828>, 2019